Synthesis, Structure, and Redox Properties of Dicopper(II,II) Complexes of *N*-(2-Hydroxyphenyl)salicylamide and Homologues. Facile Oxidation to Dicopper-(II,III) and -(III,III) Species; Crystal Structure of Bis(tetrabutylphosphonium) Bis{[(2-oxidobenzoyl)(2′-oxidophenyl)amido(3−)-*NO*^{2},μ-*O*$^{2'}$]cuprate(II)}†

Masayuki Koikawa, Hisashi Ōkawa,* Naohide Matsumoto, Mikio Gotoh, Sigeo Kida, and Takamitsu Kohzuma
Department of Chemistry, Faculty of Science, Kyushu University, Hakozaki, Higashiku, Fukuoka 812, Japan

Binuclear copper (II) complexes of *N*-(2-hydroxyphenyl)salicylamide (H_3L^1) and its homologues with a substituent on the '2-hydroxyphenyl' moiety (5-Me, H_3L^2; 5-Cl, H_3L^3; 5-NO_2, H_3L^4) have been obtained as tetrabutylphosphonium salts $[PBu_4]_2[Cu_2L_2]$. The structure of $[PBu_4]_2[Cu_2L^1{}_2]$ was solved by single-crystal *X*-ray crystallography, which demonstrated that two copper ions are bridged by the phenolic oxygen of the 'aminophenol' moiety with a Cu ··· Cu separation of 3.035(2) Å. Each copper ion adopts an essentially planar configuration, and the Cu–O and Cu–N bond distances involving the salicylamide moiety are relatively short [1.838(6) and 1.915(6) Å respectively]. Cryomagnetic investigations (80—300 K) revealed a significant antiferromagnetic spin exchange though the bridging oxygen, the $2J$ value (energy separation between the spin singlet and triplet states) being −393.4 to −448.8 cm^{-1}. The cyclic voltammogram of each complex showed two oxidation waves attributable to $Cu_2^{II,II}$–$Cu_2^{II,III}$ and $Cu_2^{II,III}$–$Cu_2^{III,III}$ processes at significantly low potentials. The dicopper(II,III) species of the L^2 complex was generated by electrochemical and chemical (with Br_2) oxidation and identified by e.s.r. investigations. The mixed-valence complex in dichloromethane showed an e.s.r. signal with a four-line hyperfine structure ($A_{av.} = 79 \times 10^{-4}$ cm^{-1}) at $g = 2.10$ at room temperature, indicating that the unpaired electron is localized on one of the copper ions on the e.s.r. time-scale. The mixed-valence complexes each showed an intense absorption in the visible region which is tentatively assigned to the intervalence transitions.

The oxidation–reduction chemistry of binuclear copper(II) complexes is the subject of many recent studies.[1–9] Interest in this area concerns attempts to mimic the active sites of some cuproproteins, to examine the mutual influence of two metal centres on the redox properties, and to gain an insight into mixed-valence species which may be formed by one-electron oxidation or reduction. Much effort has been directed to the chemical or electrochemical reduction of binuclear copper(II) complexes.[1–9] In general, mixed-valence dicopper(I,II) complexes were obtained by one-electron reduction, and electron delocalization over a pair of copper ions was evidenced by e.s.r. spectroscopy in quite a few cases.[1,3]

Characterized dicopper-(II,III) and -(III,III) complexes, on the other hand, are still very limited. Recently, Mandal *et al.*[5] reported that the dicopper(II,II) complex of a saturated macrocycle was oxidized stepwise to dicopper-(II,III) and then to -(III,III) species. Based on e.s.r. spectra, the mixed-valence species was shown to be 'spin-trapped' even at room temperature. One-electron oxidation of trinuclear copper(II) complexes of pyridine-2-carbaldehyde oxime or isonitrosoketimines to tricopper(II,II,III) species is also known.[10] Except for these two, however, there is no report on mixed-valence species involving copper(III).

In previous studies[11,12] we have shown that *N*-(2-hydroxyphenyl)salicylamide (H_3L^1) and homologues with a substituent on the '2-hydroxyphenyl' moiety function as both strong σ and π donors with the deprotonated phenolic oxygens and amide nitrogen to stabilize metal ions in higher oxidation states such as Mn^{4+}, Mn^{5+}, and Co^{4+}. These ligands bear a structural resemblance to 2-(salicylideneamino)phenol[13] and related tridentate ligands,[14] which form O-bridged dicopper(II) complexes, and are expected to act as tridentate chelates to afford binuclear copper complexes bridged by one of the phenolic oxygens. In the hope of obtaining dicopper-(II,III) and -(III,III) complexes, we have carried out investigations using H_3L^1—H_3L^4. This paper describes the synthesis and structure of dicopper(II,II) complexes, $[PBu_4]_2[Cu_2L_2]$ (L = L^1—L^4), and chemical and electrochemical oxidations to the dicopper-(II,III) and -(III,III) species.

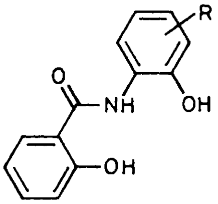

	R
H_3L^1	H
H_3L^2	5-Me
H_3L^3	5-Cl
H_3L^4	5-NO_2
H_3L^5	4-NO_2

---

† *Supplementary data available:* see Instructions for Authors, *J. Chem. Soc., Dalton Trans.*, 1989, Issue 1, pp. xvii—xx.

Table 1. Analytical data for the dicopper(II,II) complexes

	Found (%)				Calc. (%)			
Complex	C	H	N	Cu	C	H	N	Cu
$[PBu_4]_2[Cu_2L^1{}_2]$	63.30	8.00	2.65	11.6	63.40	8.10	2.55	11.4
$[PBu_4]_2[Cu_2L^2{}_2]$	63.60	8.15	2.65	11.3	64.00	8.25	2.50	12.0
$[PBu_4]_2[Cu_2L^3{}_2]$	59.45	7.30	2.45	10.9	59.70	7.45	2.40	11.3
$[PBu_4]_2[Cu_2L^4{}_2]$	59.05	7.35	4.75	10.7	58.60	7.30	4.70	11.2

Table 2. Positional parameters ($\times 10^4$) of non-hydrogen atoms of $[PBu_4]_2[Cu_2L^1{}_2]$

Atom	x	y	z
Cu	2 716(0)	3 429(1)	4 623(1)
O(1)	2 868(2)	2 301(6)	5 522(3)
O(2)	2 532(2)	4 495(6)	3 749(3)
O(3)	3 972(2)	4 679(7)	5 026(4)
N	3 348(2)	3 699(7)	5 028(4)
C(1)	3 312(3)	2 118(8)	5 923(5)
C(2)	3 490(3)	1 272(9)	6 564(5)
C(3)	3 946(3)	1 116(10)	6 941(5)
C(4)	4 219(3)	1 805(11)	6 693(6)
C(5)	4 053(3)	2 656(10)	6 072(6)
C(6)	3 593(3)	2 849(8)	5 671(5)
C(7)	3 558(3)	4 567(9)	4 754(5)
C(8)	3 270(3)	5 431(8)	4 085(5)
C(9)	3 506(3)	6 412(9)	3 899(6)
C(10)	3 311(3)	7 253(10)	3 283(6)
C(11)	2 858(3)	7 164(9)	2 820(5)
C(12)	2 611(3)	6 205(9)	2 984(5)
C(13)	2 807(3)	5 343(8)	3 631(5)
P	6 257(1)	3 813(3)	2 823(2)
C(14)	6 782(3)	4 624(9)	3 214(6)
C(15)	7 160(3)	3 925(9)	3 886(5)
C(16)	7 607(3)	4 579(9)	4 097(6)
C(17)	7 974(3)	3 960(10)	4 796(6)
C(18)	6 109(3)	3 322(11)	3 619(6)
C(19)	5 691(3)	2 513(11)	3 395(6)
C(20)	5 615(3)	2 056(13)	4 076(6)
C(21)	5 206(3)	1 247(12)	3 888(7)
C(22)	6 280(3)	2 324(10)	2 315(6)
C(23)	6 411(4)	2 505(11)	1 646(6)
C(24)	6 396(3)	1 210(11)	1 206(6)
C(25)	5 950(4)	653(14)	785(7)
C(26)	5 870(4)	5 071(13)	2 201(7)
C(27)	5 467(5)	4 728(15)	1 704(9)
C(28)	5 151(4)	5 842(17)	1 299(10)
C(29)	5 236(4)	6 799(16)	917(9)

Experimental

Materials.—All the chemicals were reagent grade and used as received. All solvents were purified before use. Dichloromethane for electrochemical measurements was dried over $MgSO_4$ and distilled under nitrogen. The electrolyte tetrabutylammonium perchlorate was recrystallized three times from a mixture of ethyl acetate and hexane and dried *in vacuo*. The ligands H_3L^1—H_3L^4 were obtained as described previously.[11]

Preparation of $[PBu_4]_2[Cu_2L_2]$ ($L = L^1$—L^4).—All the complexes were obtained in nearly the same way. The synthesis of the L^1 complex is described. A solution of H_3L^1 (460 mg), potassium t-butoxide (1 150 mg), and copper(II) acetate monohydrate (400 mg) in methanol (20 cm^3) was stirred overnight at room temperature under nitrogen. To the resulting green solution was added a methanolic solution of tetrabutylphosphonium bromide (680 mg), and the mixture was stirred for 3 h. It was evaporated to dryness under reduced pressure, the residue was dissolved in acetonitrile, and the solution passed through an alumina column (10 cm × 2 cm). The collected effluent was concentrated to 10 cm^3 and allowed to stand for a few days. The deep green crystals thus formed were collected by suction filter and recrystallized from dichloromethane. The yields of the complexes were 35—47%.

Analytical data for the complexes are given in Table 1.

X-Ray Crystal Structure Analysis of $[PBu_4]_2[Cu_2L^1{}_2]$.—On prolonged standing of a dichloromethane solution of the L^1 complex, deep green crystals of $[PBu_4]_2[Cu_2L^1{}_2]$ were obtained. A crystal of dimensions 0.40 × 0.35 × 0.55 mm was used for the *X*-ray analysis. The unit-cell parameters and intensities were measured on a Rigaku AFC-5 automated four-circle diffractometer with graphite-monochromated Mo-K_α radiation ($\lambda = 0.710\,69$ Å) at room temperature (20 °C). The data were corrected for Lorentz and polarization effects, but not for absorption.

Crystal data. $C_{28}H_{44}CuNO_3P$, $M = 537.16$, monoclinic, space group $C2/c$, $a = 32.866(15)$, $b = 10.227(3)$, $c = 18.553(8)$ Å, $\beta = 114.23(3)°$, $U = 5\,684.2$ Å^3, $Z = 8$, $D_c = 1.255$ g cm^{-3}, $F(000) = 2\,296$, $\mu(Mo\text{-}K_\alpha) = 8.51$ cm^{-1}, scan mode 2θ-ω, scan speed 6° min^{-1}, scan width $(1.2 + 0.35 \tan\theta)°$, 2θ range 2.5—42°, octant measured $+h, \pm k, \pm l$, 2 774 reflections with $|F_o| > 3\sigma(|F_o|)$, equal weight of $w = 1$ for all 3 574 reflections, $R = 0.0669$, $R' = 0.0715$.

The structure was solved by direct and Fourier difference methods and refined by block-diagonal least squares. The hydrogen atoms were included in the structure-factor calculation, but their parameters were not refined. The atomic scattering factors were taken from ref. 15. All the calculations were performed on a Facom M-780 computer at the Computer Center of Kyushu University by the use of a local version[16] of the UNICS-III[17] and ORTEP[18] programs. The final positional parameters of non-hydrogen atoms are given in Table 2.

Additional material available from the Cambridge Crystallographic Data Centre comprises H-atom co-ordinates and thermal parameters.

Physical Measurements.—Analytical data for carbon, hydrogen, and nitrogen were obtained at the Elemental Analysis Service Center, Kyushu University. Copper analyses were performed on a Nippon Jarrel-Ash AA781 atomic absorption and flame emission spectrophotometer. Infrared spectra were recorded on a JASCO IR model 810 spectrometer on KBr discs or Nujol mulls, electronic spectra on a Shimadzu model MPS-5000 Multipurpose spectrophotometer in dichloromethane. Magnetic susceptibilities were determined on powder samples in the temperature range 80—300 K, with a Faraday balance designed in our laboratory. The apparatus was calibrated using $[Ni(en)_3]S_2O_3$ (en = ethylenediamine).[19] Diamagnetic corrections for the constituent atoms were made by the use of Pascal's constants. *X*-Band e.s.r. spectra were recorded on a JES-ME-3 spectrometer. Cyclic voltammograms (c.v.s) and differential pulse polarograms (d.p.p.s) were measured in dichloromethane solutions containing NBu_4ClO_4 (0.1 mol dm^{-3}) as the supporting electrolyte with a Yanagimoto P-1000 voltammetric analyser. A three-electrode cell was used, equipped with a glassy carbon working electrode, a platinum coil as the auxiliary electrode, and a calomel reference electrode.

Results and Discussion

Structure of $[PBu_4]_2[Cu_2L^1{}_2]$.—An ORTEP plot of the anion $[Cu_2L^1{}_2]^{2-}$ is given in Figure 1, together with the atom numbering system. Relevant bond distances and angles with their estimated standard deviations (e.s.d.s) are given in Table 3.

The anion has the expected binuclear structure with an inversion centre. Two possible bridging modes were considered

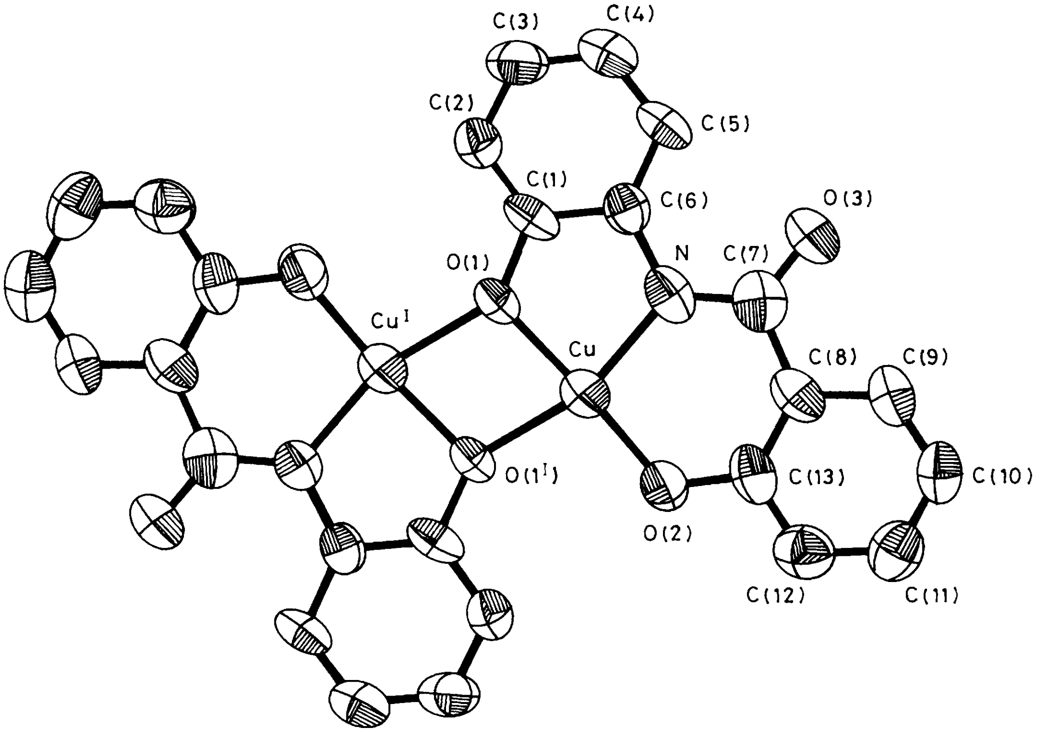

Figure 1. ORTEP view of the anion $[Cu_2L^1{}_2]^{2-}$ with the atom numbering system

Table 3. Relevant bond distances (Å) and angles (°)

Cu–O(1)	1.916(6)	Cu–O(2)	1.838(6)
Cu–O(1^{I})	1.971(5)	Cu–N	1.915(6)
C(1)–O(1)	1.353(8)	C(1)–C(2)	1.389(11)
C(1)–C(6)	1.409(13)	C(2)–C(3)	1.377(12)
C(3)–C(4)	1.359(16)	C(3)–C(4)	1.365(14)
C(5)–C(6)	1.397(11)	C(6)–N	1.426(9)
C(7)–N	1.344(13)	C(7)–O(3)	1.247(10)
C(9)–C(10)	1.361(13)	C(10)–C(11)	1.383(12)
C(11)–C(12)	1.384(14)	C(12)–C(13)	1.413(11)
C(13)–C(8)	1.406(10)	C(13)–O(2)	1.333(11)
Cu ⋯ Cu^{I}	3.035(2)		
O(1)–Cu–N	83.9(2)	O(2)–Cu–N	99.8(2)
O(1)–Cu–O(1^{I})	77.3(5)	O(2)–Cu–O(1^{I})	96.0(5)
Cu–O(1)–Cu^{I}	102.6(5)	Cu–O(1^{I})–C(1^{I})	141.4(5)
Cu–O(1)–C(1)	113.4(5)	Cu–O(2)–C(13)	122.0(4)
Cu–N–C(6)	112.8(5)	Cu–N–C(7)	126.0(5)
O(1)–Cu–O(2)	176.1(2)	O(1^{I})–Cu–N	161.1(5)

Symmetry related position: I $-x + \frac{1}{2}, -y + \frac{1}{2}, 1 - z$.

for the present complexes, *i.e.* through the phenolic oxygen of the salicylamide moiety or through the phenolic oxygen of the aminophenol moiety. The *X*-ray result clearly demonstrates that the phenolic oxygen of the aminophenol moiety functions as a bridge with the Cu ⋯ Cu separation of 3.035(2) Å. Each copper ion adopts an essentially planar configuration with the bridging phenolic oxygens O(1) and O(1^{I}), the non-bridging phenolic oxygen O(2), and the deprotonated amide nitrogen. The Cu–O(1) distance differs considerably from Cu–O(1^{I}) [1.916(6) and 1.971(5) Å, respectively]. The Cu–N and Cu–O(2) distances are 1.915(6) and 1.838(6) Å, respectively. It should be emphasized that, except for Cu–O(1^{I}), the bond distances are significantly short compared with those of related complexes.[20,21] In particular, the Cu–O(2) distance is unusually short and comparable to those of copper(III) complexes.[22,23] Such short Cu–O and Cu–N bonds are expected to contribute to the stabilization of higher-oxidation-state species, dicopper(II,III) and -(III,III). The configuration around the bridging oxygen is highly distorted from sp^2 hybridization: the C(1)–O(1)–Cu angle is only 113.4(5)° whereas C(1)–O(1)–Cu^{I} [Cu–O(1^{I})–C(1^{I})] is 141.4(5)°. The angle Cu–O(1)–Cu^{I} [102.6(5)°] is normal for doubly O-bridged dicopper(II) complexes.

Electronic Spectra.—Electronic spectra of the complexes in dichloromethane obey Beer's law in the concentration range 1×10^{-3}—1×10^{-4} mol dm^{-3}, indicating that the binuclear structure is stable in solution. The electronic spectra of the L^1 and L^4 complexes are given in Figure 2, and the numerical data are summarized in Table 4. The L^1 complex shows three absorption bands in the visible region. The very intense band at 30 600 cm^{-1} may be attributed to an intraligand or a charge-transfer transition. The band at 16 800 cm^{-1} and a discernible shoulder near 22 000 cm^{-1} may be assigned to *d–d* transitions. The L^2 and L^3 complexes show similar spectral features. The splitting of *d* orbitals in square-planar copper(II) complexes was discussed comprehensively by Nishida and Kida[24] in terms of the effect of π bonding with ligands. In general, copper(II) complexes of strongly π-basic ligands show a large splitting of *d–d* bands while complexes of π-acidic or π-neutral ligands show a small splitting of *d–d* bands. The splitting of *d–d* bands in the L^1—L^3 complexes is very large and indicative of the strongly π-basic character of the ligands. This is in accord with our previous finding that H_3L^1—H_3L^5 can stabilize higher oxidation states of manganese and cobalt ions. The electronic spectrum of the L^4 complex is characterized by another intense absorption band at 23 500 cm^{-1} (log ε 4.54), attributable to an intraligand transition associated with the nitro group.[11] Splitting of *d–d* bands should also occur in this complex, though the band position of the higher *d–d* component is obscured by the intra-ligand band.

Magnetic Properties.—All the complexes show a subnormal magnetic moment ($\mu_{eff.}$ per Cu = 1.06—1.29 μ_B) at room

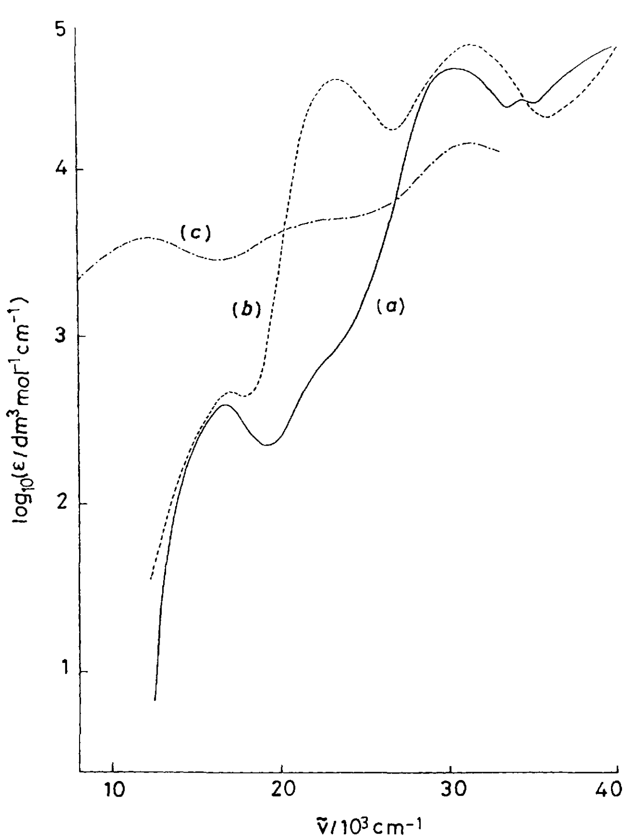

Figure 2. Electronic spectra in dichloromethane: (*a*) $[PBu_4]_2[Cu_2L^1{}_2]$, (*b*) $[PBu_4]_2[Cu_2L^4{}_2]$, and (*c*) the dicopper(II,III) complex of L^1 generated by electrochemical oxidation at +0.40 V *vs.* saturated calomel electrode (s.c.e.)

Table 4. Electronic spectral data for dicopper(II,II) complexes[a]

Complex	$\tilde{\nu}/10^3$ cm^{-1} (log ε)			
$[PBu_4]_2[Cu_2L^1{}_2]$	16.8(2.59)	22(≈2.7)[b]		30.6(4.62)
$[PBu_4]_2[Cu_2L^2{}_2]$	16.9(2.68)	22(≈2.8)[b]		30.4(4.63)
$[PBu_4]_2[Cu_2L^3{}_2]$	16.8(2.65)	22(≈2.8)[b]		30.0(4.60)
$[PBu_4]_2[Cu_2L^4{}_2]$	17.2(2.67)	—	23.5(4.54)	31.4(4.75)

[a] In dichloromethane. [b] Shoulder.

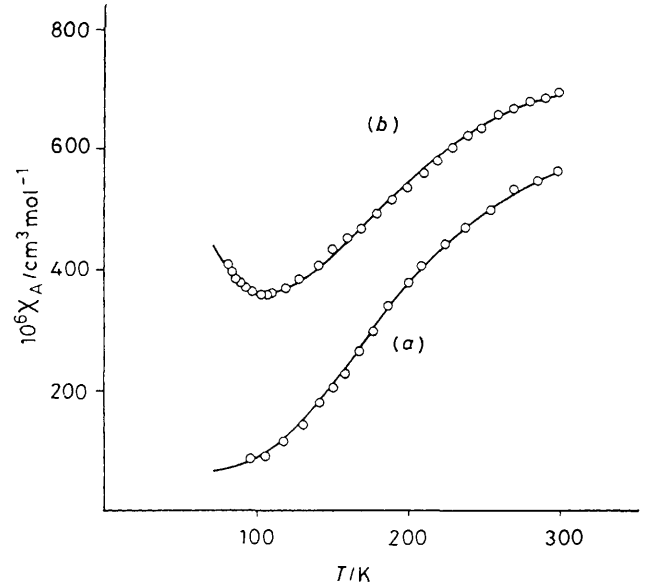

Figure 3. Temperature variations of the magnetic susceptibility of (*a*) $[PBu_4]_2[Cu_2L^1{}_2]$ and (*b*) $[PBu_4]_2[Cu_2L^4{}_2]$. The solid curves are based on equation (1) and the magnetic parameters in Table 5

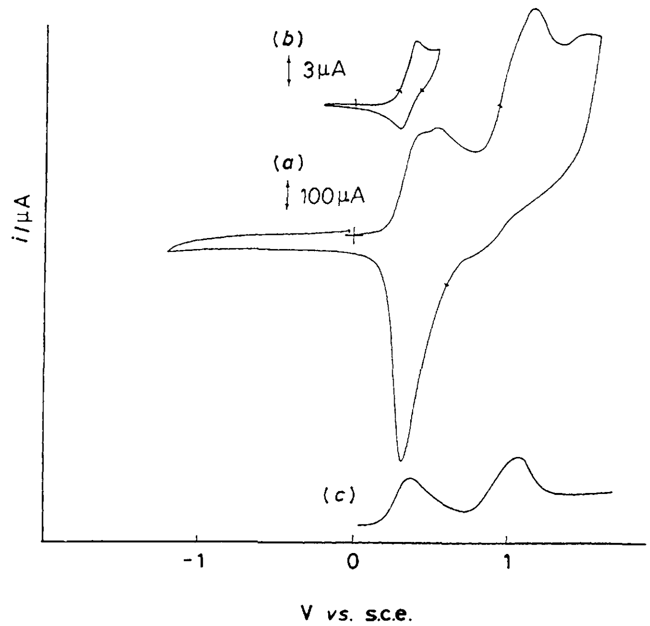

Figure 4. Cyclic voltammograms [(*a*) and (*b*)] and differential pulse polarogram [(*c*)] of $[PBu_4]_2[Cu_2L^2{}_2]$ in CH_2Cl_2, glassy carbon electrode, scan speed 80 mV s^{-1}. Trace (*b*) was obtained only for the first wave

temperature, suggesting an intramolecular antiferromagnetic interaction through the bridging phenolic oxygens. The magnetic susceptibilities were determined over the range from room temperature to liquid-nitrogen temperature. The χ_A *vs.* T curves for the L^1 and L^4 complexes are given in Figure 3 (*a*) and (*b*), respectively. For the L^1 complex the susceptibility decreases with decreasing temperature and approaches *ca.* 60 × 10^{-6} cm^3 mol^{-1} (temperature-independent paramagnetism) below 100 K. In the case of the L^4 complex the susceptibility also decreases with decreasing temperature down to 355 × 10^{-6} cm^3 mol^{-1} at *ca.* 110 K but increases again below this temperature. Such a magnetic behaviour is characteristic of antiferromagnetically coupled dicopper(II,II) containing a small amount of paramagnetic contaminant. Thus, the magnetic analyses were carried out with the Bleaney–Bowers[25] equation (1) based on the isotropic Heisenberg model ($\mathcal{H} = -2JS_1S_2$), including a correction term for monomeric copper(II) species as the contaminant where p is the mole fraction of the paramagnetic contaminant and other symbols have their usual meanings. As

$$\chi_A = (Ng^2\beta^2/3kT)\{1 + [\exp(-2J/kT)]/3\}^{-1}(1-p) + 0.45p/T + N_\alpha \quad (1)$$

indicated by Figure 3 the cryomagnetic properties can be well simulated with the above equation, and the results demonstrate the operation of a significant antiferromagnetic spin coupling in the present complexes. The magnetic parameters thus determined are summarized in Table 5.

Electrochemistry.—C.v.s and d.p.p.s were determined on a glassy carbon electrode in dichloromethane, and typical examples are shown in Figure 4. In general two irreversible

Table 5. Magnetic data for dicopper(II,II) complexes

Complex	$\mu_{eff.}/\mu_B$ [a]	g	J/cm^{-1}	$10^6 N\alpha$/cm^3 mol^{-1}	p [b]
$[PBu_4]_2[Cu_2L^1{}_2]$	1.18	2.15	−224.4	60	0
$[PBu_4]_2[Cu_2L^2{}_2]$	1.06	2.21	−206.9	60	0.01
$[PBu_4]_2[Cu_2L^3{}_2]$	1.28	2.20	−196.7	60	0.01
$[PBu_4]_2[Cu_2L^4{}_2]$	1.29	2.24	−216.6	60	0.058

[a] Moment per copper at room temperature. [b] Mole fraction of mononuclear impurity.

oxidation waves were found at positive potential [see trace (*a*)] but no wave at negative potential down to −2.0 V. When measured only for the first oxidation, on the other hand, each c.v. showed much improved reversibility. Based on controlled-potential electrolysis, this wave was shown to involve one-electron transfer. For the second wave, however, the number of electrons transferred could not be determined probably because of partial decomposition upon electrolysis at the second potential. Since the free ligands (sodium salts) show no electrochemical response up to +1.3 V, we tentatively assign the two waves to the oxidation processes (2) and (3) at the metal centre.

$$Cu_2{}^{II,II} \overset{E_{\frac{1}{2}}(1)}{\rightleftharpoons} Cu_2{}^{II,III} \qquad (2)$$

$$Cu_2{}^{II,III} \overset{E_{\frac{1}{2}}(2)}{\rightleftharpoons} Cu_2{}^{III,III} \qquad (3)$$

The validity of the assignment is supported by e.s.r. measurements as mentioned later. For the first wave the potential determined by c.v. was adopted but for the second wave the potential determined by d.p.p. was tentatively taken as the formal redox potential. The results are summarized in Table 6. It should be emphasized that both the first and second oxidation potentials are extremely low. The very facile oxidation to the dicopper-(II,III) and -(III,III) species can be ascribed to the strong donating ability of the ligands, and this is in accord with the *X*-ray structural and electronic spectral results discussed above. Further, it is seen from Table 6 that the first potential shifts to lower values when the substituent becomes more electron-donative. A similar trend has been observed for the cobalt and manganese complexes of H_3L^1—H_3L^5.[5,11,12]

The stability of the mixed-valence dicopper(II,III) species can be expressed in terms of the conproportionation constant K_{con} [equation (4)] which can be determined electrochemically

$$Cu_2{}^{II,II} + Cu_2{}^{III,III} \xrightarrow{K_{con}} 2\,Cu_2{}^{II,III} \qquad (4)$$

from $K_{con} = \exp(\Delta E/0.0591)$ (at 25 °C), where $\Delta E = E_{\frac{1}{2}}(1) - E_{\frac{1}{2}}(2)$.[4a] The K_{con} values for the L¹ and L² complexes were evaluated and the results are included in Table 6. The values observed are very large ($>10^{11}$) and indicate high stability of the mixed-valence state relative to the dicopper-(II,II) and -(III,III) states. For the dicopper(II,III) complex of a macrocyclic ligand a much smaller K_{con} value (5.2×10^3) was reported.[5]

E.S.R. and Visible Spectra of Dicopper(II,III) *Species.*—The mixed-valence species of the L² complex, generated chemically or electrochemically, was studied by means of *X*-band e.s.r. spectroscopy. The dicopper(II,II) species is e.s.r.-silent in accord with the strong antiferromagnetic spin-exchange interaction found for this complex. When it was oxidized with 0.5 molar equivalent of bromine in dicholoromethane the solution assumed an intense red colour and showed an e.s.r. signal with a four-line hyperfine structure ($A_{iso} = 79.7 \times 10^{-4}$ cm^{-1}) centred at $g = 2.10$ at room temperature [see Figure 5(*a*)]. This spectral feature is characteristic of a single unpaired electron of a mixed-valence complex localized on one of the copper centres on the e.s.r. time-scale.[2,3,5] Further addition of bromine resulted in a decrease in the e.s.r. signal, which practically disappeared when $Cu_2{}^{II,II}/Br_2 = 1:1$ [Figure 5(*b*)]. This is consistent with the generation of a dicopper(III,III) complex according to reaction (5). When the L² complex was oxidized electrochemically

$$Cu_2{}^{II,II} + Br_2 \longrightarrow Cu_2{}^{III,III} + 2\,Br^- \qquad (5)$$

at +0.35 V the solution assumed a brown colour and gave essentially the same e.s.r. spectrum as trace (*a*) in Figure 5.

For the frozen solutions of the mixed-valence species (liquid-nitrogen temperature) the e.s.r. spectral feature is 'rhombic' [Figure 5 (*c*)], irrespective of the manner of oxidation. E.s.r. parameters evaluated from the spectra are $g_z = 2.23$ ($A_z = 177 \times 10^{-4}$ cm^{-1}), $g_y = 2.05$ ($A_y = 20 \times 10^{-4}$ cm^{-1}), and $g_x = 2.02$. The spectra are similar to those of spin-trapped dicopper(I,II) complexes,[1b,3] except that in the latter cases the splitting of the g_x and g_y components is generally small and the spectra can be regarded as of 'axial symmetry.' The rhombic e.s.r. feature of the present dicopper(II,III) complex may be attributed to the significantly unsymmetrical surroundings about each copper ion, *i.e.* different donor-atom sets and different copper–ligand bonds along the *x* and *y* axes.

The mixed-valence species of the L¹ and L² complexes, generated by electrochemical oxidations, were sufficiently stable at ambient temperature to allow electronic spectral investigations. The spectrum of the mixed-valence species of the L¹ complex is included in Figure 2 [trace (*c*)]. In this case a very intense absorption band appeared at 12.2×10^3 cm^{-1} (3 890 dm³ mol^{-1} cm^{-1}). The corresponding band for the mixed-valence species of the L² complex is located at 15.3×10^3 cm^{-1} and its absorption coefficient is 2 140 dm³ mol^{-1} cm^{-1}. We tentatively assign the low-energy band found for these dicopper(II,III) complexes to the intervalence transition band ($Cu^{II} \longrightarrow Cu^{III}$). A very similar absorption band has been found for the tricopper(II,II,III) complexes of isonitrosoketimines[10] and the band at 12×10^3 cm^{-1} (1 000 dm³ mol^{-1} cm^{-1}) was assigned to the intervalence transition band. The mixed-valence species of the L³ and L⁴ complexes were unstable at room temperature and their intervalence transition was observed as a weaker band (200 dm³ mol^{-1} cm^{-1}) near 15×10^3 cm^{-1}.

Table 6. Electrochemical data (*E* values in V) [a]

	Wave I			Wave II		
Complex	E_{p_a}	E_{p_c}	$E_{\frac{1}{2}}(1)$ [b]	$E_{\frac{1}{2}}(2)$ [c]	ΔE [d]	K_{con}
$[PBu_4]_2[Cu_2L^1{}_2]$	0.42	0.33	0.38	1.08	0.70	7.0×10^{11}
$[PBu_4]_2[Cu_2L^2{}_2]$	0.37	0.29	0.33	1.02	0.69	4.7×10^{11}
$[PBu_4]_2[Cu_2L^3{}_2]$	0.51	0.42	0.47	—		
$[PBu_4]_2[Cu_2L^4{}_2]$	0.77	0.62	0.70	—		

[a] Determined in CH_2Cl_2, glassy carbon electrode, scan rate 80 mV s^{-1}. [b] $Cu_2{}^{II,II}$–$Cu_2{}^{II,III}$. [c] $Cu_2{}^{II,III}$–$Cu_2{}^{III,III}$, determined by d.p.p. [d] $\Delta E = E_{\frac{1}{2}}(1)-E_{\frac{1}{2}}(2)$.

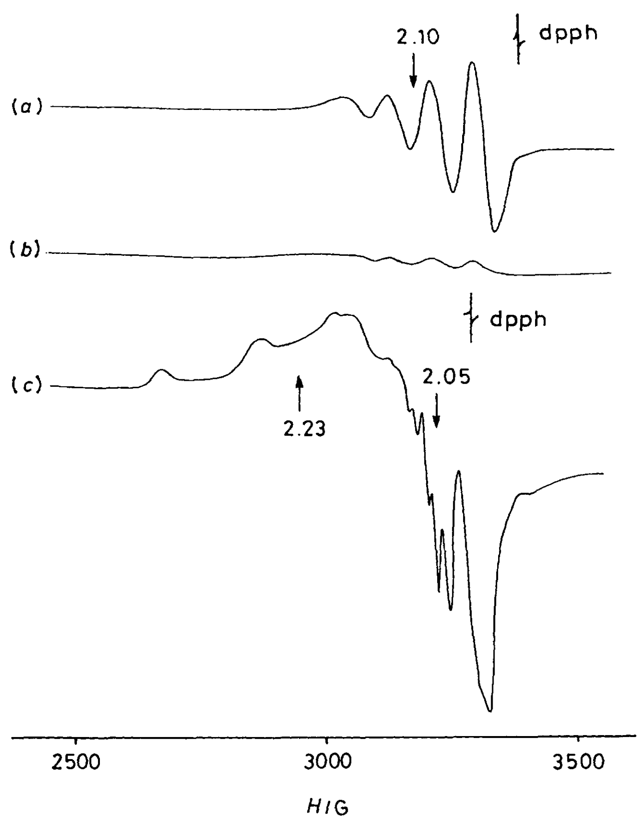

Figure 5. *X*-Band e.s.r. spectra of the dicopper(II,III) species of the L^2 complex generated by bromine oxidation: (*a*) $Cu_2^{II,II}/Br_2 = 2:1$, at room temperature; (*b*) $Cu_2^{II,II}/Br_2 = 2:2$, at room temperature; (*c*) frozen solution of (*a*) at liquid-nitrogen temperature. Similar spectra were obtained for the mixed-valence species generated by electrochemical oxidation at +0.35 V. dpph = Diphenylpicrylhydrazyl; G = 10^{-4} T

Acknowledgements

We appreciate helpful discussions with Associate Professor T. Isobe of Kyushu University. This work was partially supported by a grant-in-aid for scientific research (No. 63470041) from the Ministry of Education, Science and Culture, Japan.

References

1 (*a*) R. R. Gagne, C. A. Koval, and T. J. Smith, *J. Am. Chem. Soc.*, 1977, **99**, 8367; (*b*) R. R. Gagne, C. A. Koval, T. J. Smith, and M. C. Cimolino, *ibid.*, 1979, **101**, 4571; (*c*) R. R. Gagne, L. M. Henling, and T. J. Kistenmacher, *Inorg. Chem.*, 1980, **19**, 1226; (*d*) R. R. Gagne, C. L. Spiro, T. J. Smith, C. A. Hamann, W. R. Thies, and A. K. Shiemke, *J. Am. Chem. Soc.*, 1981, **103**, 4073.

2 A. W. Addison, *Inorg. Nucl. Chem. Lett.*, 1976, **12**, 899.

3 R. C. Long and D. N. Hendrickson, *J. Am. Chem. Soc.*, 1983, **105**, 1513.

4 (*a*) S. K. Mandal and K. Nag, *J. Chem. Soc., Dalton Trans.*, 1983, 2429; (*b*) *ibid.*, 1984, 2141; (*c*) S. K. Mandal, B. Adhikary, and K. Nag, *ibid.*, 1986, 1175.

5 S. K. Mandal, L. K. Thompson, K. Nag, and J. P. Charland, *Inorg. Chem.*, 1987, **26**, 1391.

6 M. Mikuriya, M. Nakamura, H. Ōkawa, and S. Kida, *Chem. Lett.*, 1982, 839.

7 T. Izumitani, M. Nakamura, H. Ōkawa, and S. Kida, *Bull. Chem. Soc. Jpn.*, 1982, **55**, 2122.

8 J. P. Gisselbrecht, M. Gross, A. H. Alberts, and J. M. Lehn, *Inorg. Chem.*, 1980, **19**, 1386.

9 D. E. Fenton and R. L. Lintvedt, *J. Am. Chem. Soc.*, 1978, **100**, 6367; R. L. Lintvedt and L. S. Kramer, *Inorg. Chem.*, 1983, **22**, 796; R. L. Lintvedt, B. A. Schoenfelner, and K. A. Rupp, *ibid.*, 1986, **25**, 2704.

10 D. Datta and A. Chakravorty, *Inorg. Chem.*, 1983, **22**, 1611 and refs. therein.

11 M. Koikawa, H. Ōkawa, and S. Kida, *J. Chem. Soc., Dalton Trans.*, 1988, 641.

12 M. Koikawa, M. Gotoh, H. Ōkawa, S. Kida, and T. Kohzuma, *J. Chem. Soc., Dalton Trans.*, 1989, 1613.

13 A. P. Ginsberg, R. C. Sherwood, and E. Koubek, *J. Inorg. Nucl. Chem.*, 1967, **29**, 353.

14 U. Casellato, P. A. Vigato, and M. Vidali, *Coord. Chem. Rev.*, 1977, **23**, 31.

15 'International Tables for *X*-Ray Crystallography,' Kynoch Press, Birmingham, 1974, vol. 4.

16 S. Kawano, *Rep. Comput. Cent., Univ. Kyushu*, 1980, **13**, 39.

17 T. Sakurai and K. Kobayashi, *Rep. Inst. Phys. Chem. Res.*, 1979, **55**, 69.

18 C. K. Johnson, Report No. 3794, Oak Ridge National Laboratory, Oak Ridge, Tennessee, 1965.

19 N. F. Curtis, *J. Chem. Soc.*, 1961, 3147.

20 B. F. Hoskins, N. J. Mcleod, and H. A. Schaap, *Aust. J. Chem.*, 1976, **29**, 515.

21 H. C. Freeman, J. E. W. L. Smith, and J. C. Taylor, *Acta Crystallogr.*, 1961, **14**, 407.

22 F. C. Anson, T. J. Collins, T. G. Richmond, B. D. Santarsiero, J. E. Toth, and B. G. R. T. Treco, *J. Am. Chem. Soc.*, 1987, **109**, 2974.

23 L. L. Diaddario, W. R. Robinson, and D. W. Margerum, *Inorg. Chem.*, 1983, **22**, 1021.

24 Y. Nishida and S. Kida, *Coord. Chem. Rev.*, 1979, **27**, 275.

25 B. Bleaney and K. D. Bowers, *Proc. R. Soc. London, Ser. A*, 1952, **214**, 451.

Received 16*th January* 1989; *Paper* 9/00270G